ORIGINAL ARTICLE

Sweeping-beam technique with electrons for large treatment areas as total skin irradiation

Dosimetric and technical aspects of a modified Stanford technique

Michael Schöpe[1] · Jacob Sahlmann[1] · Kathleen Lorenz[1] · Anne Findeisen[1] · Thomas Barthel[1] ·
Gunther Klautke[1]

Abstract

Purpose Total skin electron beam therapy (TSEBT) is still a technical and therapeutic challenge today. Thus, we developed TSEBT using a sweeping-beam technique.

Methods For treatment delivery, a linear accelerator Versa HD (ELEKTA, Stockholm, Sweden) with high-dose-rate electrons (HDRE) was used with a dose rate of 9000 MU/min. Dosimetry quality assurance was performed by multiple measurements with film dosimetry, 2D array, and Roos chamber.

Results Clinical experience shows that treatment durations of 75 to 90 min are usual for the Stanford technique without using HDRE. With this new sweeping-beam irradiation technique, the total treatment time of a daily fraction could be reduced to 20 min while keeping over- and underdosing low. The treatment area is about 60 cm × 200 cm and the dose distribution is uniform within 2% and 5% in vertical and horizontal directions, respectively. Initially, the electron energy of 6 MeV is reduced to 3.2 MeV by 1-cm polymethylmethacrylat (PMMA) scatter and the irradiation conditions of a source–surface distance (SSD) of 350 cm. The photon contamination drops to under 1%.

Conclusion These results show that the mean dose to total skin varies between 1.3 and 1.8 Gy. The sweeping-beam technique with electrons has a homogeneous dose distribution in connection with a short treatment time.

Keywords Total skin electron beam therapy (TSEBT) · Total skin electron irradiation (TSEI) · Mycosis fungoides · High-dose-rate electrons · In situ film dosimetry

Introduction

Large irradiation areas with electrons are mainly required for total skin irradiation in case of diffuse involvement of cutaneous T-cell lymphoma, but also for extensive skin manifestations. In this treatment situation, a continuous and homogeneous dose distribution over the whole skin surface is required, with a low penetration depth of about 0.5 to 1 cm. In the past, single doses of 2 Gy to a total dose of 36 Gy were applied in treatment of cutaneous T-cell lym-

phoma, but nowadays, more studies with a total skin dose of 12 Gy (single dose 1.0 to 1.5 Gy) show the same good results, with response rates of up to 95% (complete remission in 33%) but significantly lower toxicity. The combination with checkpoint inhibitors also shows local and systemic synergistic effects, which is of special interest for the future [1, 2, 4, 5, 7, 10–12, 14–16, 19, 22, 23, 25, 26, 28].

Large irradiation areas with electrons usually use the so-called Stanford technique with several fixed radiation fields. In this case, in the connecting regions, too high or too low doses can occur, despite daily shifting of the border of the connecting regions [6]. Additionally, underdosing can be seen on top of the shoulders or the scalp, which must then be compensated with additional radiation fields. All these points lead to an extension of daily treatment time, which alone can be an unnecessary burden for patients.

✉ Michael Schöpe
m.schoepe@skc.de

1 Department of Radiation Oncology, Klinikum Chemnitz gGmbH, Bürgerstraße 2, 09113 Chemnitz, Germany

Therefore, a new technical approach to large-area irradiation with electrons is presented below with the corresponding dosimetry verification.

Materials and methods

Patient positioning

Patients are irradiated from three different angles for each fraction. On the first day, the irradiation runs at 0°, 120°, and 240° and on the second day, at 60°, 180°, and 300°. This allowed a relatively homogeneous dose distribution to be achieved. With the accessories for the treatment shown in Fig. 1, the patient positioning is simple and reproducible.

A special construction was built to achieve safe and reproducible positioning of the patients and also of a special setup with a plate of polymethylmethacrylat (PMMA) (Fig. 1a). Two handles were integrated, which can be varied easily both horizontally and vertically. Thus, optimum positioning of arms and the upper body of the patient can be performed reproducibly. The blue elements of polystyrene on the ground shown in Fig. 1a are used to gain height for the rotatable circular plate (Fig. 1b). This results in a higher patient position, which achieves that the patient's vertical center is on the same level as the isocenter of the linear accelerator. The entire construction was temporarily attached to the wall so that it could be safely prevented from shifting or tipping over.

Fig. 1 Patient positioning. **a** Construction for patient positioning. **b** Rotatable plate with footprints for different treatment angles. **c** Shielding of eyes. **d** Shielding of nail beds

Evaluation of shielding and scatter effects

Additional investigations to examine shielding effects of different materials have been carried out. The eyes, nail beds, and the hands often need special protection. External eye shields that are fabricated in-house are constructed with circular pieces of lead. The thickness of the lead is 4 mm. The eye shielding area was about 14 mm in diameter. The lead shielding was attached like swimming goggles with hook-and-loop tape on the head (Fig. 1c). So, it was achieved that the lead shields had close contact with the eyeballs. The nail beds of the feet were protected by custom-made 2-mm thick lead sheets (Fig. 1d). Furthermore, the shielding effect of underwear with impact of dose was investigated. For the choice of the scatter shape, some theoretical considerations were performed. The scatter material was chosen to be PMMA, as it behaves like water and reduces the mean electron energy to the desired value.

Radiation technique

In contrast to the generally known Stanford technique using two overlapping treatment fields, we developed a sweeping-beam technique [13, 18, 21, 27]. The main field, with 80% dose weight, is an arc beam over 74 degrees, namely from 233 to 307 degrees (Fig. 2). In order to achieve a homogeneous dose distribution, two additional equally weighted static fields at 307 and 233 degrees were used. The angles of the static fields correspond to the start and stop angles of the arc field. This allows a continuous irradiation process.

For treatment delivery, a linear accelerator Versa HD (ELEKTA) with high-dose-rate electrons (HDRE) was used. The dose rate of the HDRE with an energy of 6 MeV is 9000 MU/min and is passed by an open field. This high dose rate is an essential requirement to achieve a very short treatment time [20, 29, 30]. The irradiation time for the three fields is only 1.75 min. The total time for the three irradiation angles is, on average, 10 min. Most of the time was needed to change the position of the patients for the different irradiation angles. The total treatment delivery time (from entering the room to leaving the room) is only 20 min on average. The advantages of this irradiation method are the short duration of treatment and the homogeneous dose distribution.
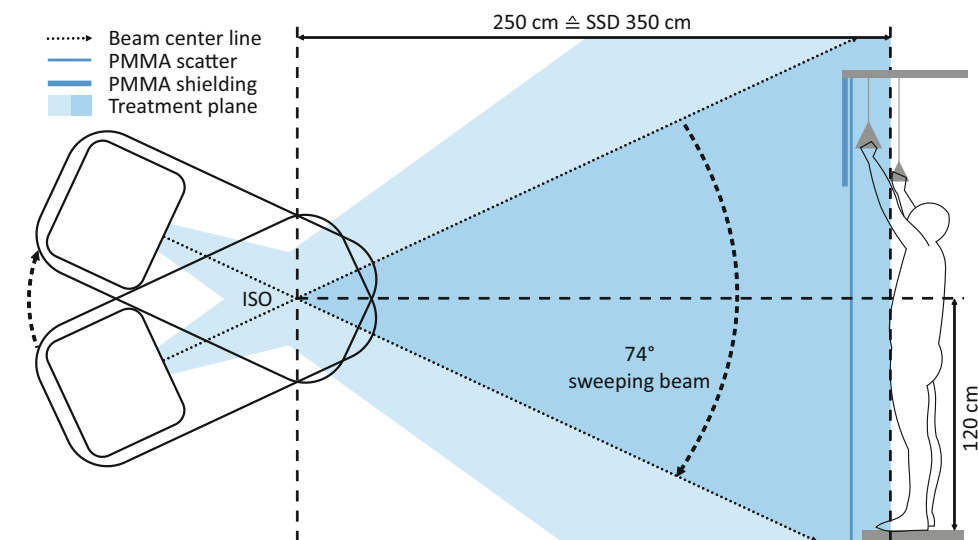
The distance from the source to the skin of the patient is 350 cm. About 15 cm in front of the patient, a 1-cm thick PMMA plate was positioned. This scatter plate causes a homogeneous dose distribution and a reduction of the electron energy.

The real dose to the skin of the patient had a relatively high range because of the complex structure of the human surface and due to the radiation technique. The prescribed dose of 2.0 Gy per fraction corresponds to the maximum skin dose typically measured in the abdominal area or on the instep of the foot.

Dosimetry

Dosimetry plays an essential role during the planning as well as during the treatment process. Due to the geometrical irradiation setup and the low electron energy, dose measurements with a water phantom were not possible. Therefore, a Roos Electron Chamber (PTW Freiburg GmbH, Freiburg, Germany), a 2D array (OCTAVIUS Detector 1500, PTW Freiburg GmbH, Freiburg, Germany), and dosimetric films (GafChromic EBT3, Ashland Advanced Materials, Bridgewater, NJ, USA) were used for dosimetry. Absolute dosimetry and calibration of the films were measured by the Roos chamber. In addition, the Roos chamber was used to measure the depth dose distribution and to optimize the irra-

Fig. 2 Treatment setup for the sweeping-beam technique

Beam center line
PMMA scatter
PMMA shielding
Treatment plane

250 cm ≙ SSD 350 cm

ISO

74° sweeping beam

120 cm

diation fields. These measurements were always performed in a PMMA-plate phantom. A calibration factor was determined for this purpose. To record dose profiles and to examine field boundaries, a 2D array was deployed. Film dosimetry not only served for determination of the patient's skin dose during irradiation, but also to measure vertical and horizontal dose profiles.

GafChromic EBT3 films were used for film dosimetry. Film pieces with a size of 3 cm × 6 cm were used for both in situ measurements at specific spots and for investigations of dose profiles. The large detector area has the advantage of a relatively high statistical certainty of the measurement results. In some cases of the in situ measurement, the films couldn't be attached evenly to the patient, so that parts of the area didn't have direct contact to the skin. Thus, an additional uncertainty in the measurement results can't be excluded. It was also important for the evaluation of the films to keep a constant time between exposure and readout of the films. The delay was 24 h each. Analysis of the films was executed with an Epson Scanner Expression 11000 XL (Epson, Suwa, Japan). Pixel values (PV) were extracted by the software PTW FilmCal. The value of the net optical density (ODNet), which is needed for dose determination, is calculated by using:
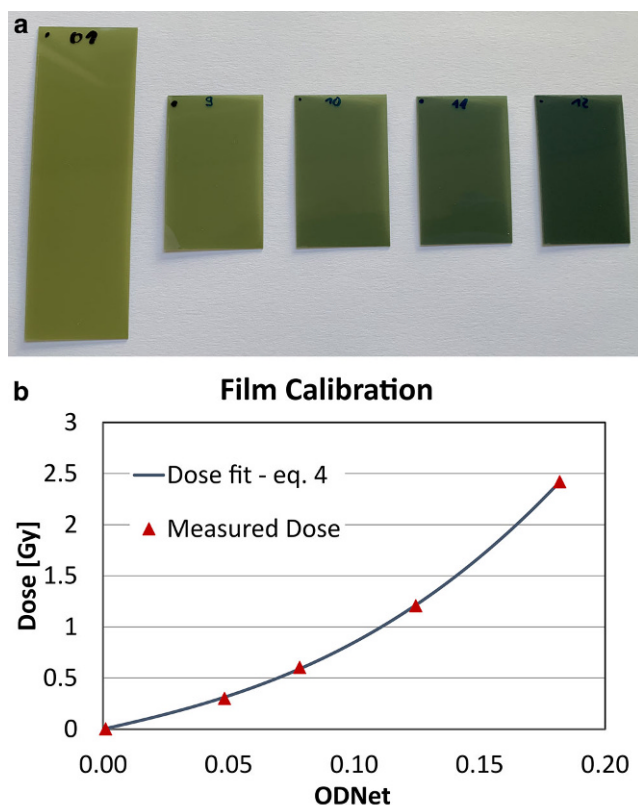
$$OD_{\mathrm{NET}} = \log_{10} \frac{PV_{\mathrm{irradiated}}}{PV_{\mathrm{unirradiated}}} \qquad (1)$$

Every film sheet, which was split into pieces of 3 cm × 6 cm, was calibrated using the Roos chamber to further reduce the measurement uncertainty of film dosimetry. A calibration curve can be generated from irradiated films of known dose (see Fig. 3a). It was revealed that films of different charges can deviate by up to 10% if they are used with the same calibration curve. Consequently, calibration of the film sheets is necessary to prevent additional systematic faults. The correlation of the ODNet values and dose (D) results from following formula:

$$D = a \cdot OD_{\mathrm{NET}} + b \cdot OD_{\mathrm{NET}}{}^{c} \qquad (2)$$

Fig. 3b shows a typical calibration curve which indicates a good correlation between ODNet values and measured dose for this method. The uncertainty of dose determination can be declared as approximately 3%.

Results

Shielding effects

Shielding effects of lead, PMMA, and textile underwear were investigated. Experiments show that 2 mm of lead reduces the dose to nearly 0% under the given treatment conditions. The hands had no symptoms of the disease. For protection of the hands, a 3-cm PMMA plate was used. This reduced the dose almost completely.

There is always a discussion regarding whether irradiation with underwear entails underdosing or whether this is possible in the interests of the patient's comfort [8, 24]. Thus, the shielding effect of textile underwear was investigated in detail. For this purpose, phantom measurements with different textiles were carried out. The shielding effect is approximately only 2% on average. The maximum dose reduction occurs with tangential irradiation, but does not exceed 20%. This could be confirmed by the in situ measurements. Taking the relatively wide value range of the actually achieved skin dose into account, the shielding effect of underwear can be neglected. Wearing a light nonwired jogging bra has the advantage of keeping the female patient's breasts reproducibly at the same position. Furthermore, the shadowed area of the inframammary fold was reduced.

Fig. 3 Film dosimetry. **a** Irradiated films of known dose for calibration of a film sheet. **b** Calibration curve of a film sheet

Scatter effect

The following considerations examine the difference between two versions of scatter close to the patient's body: PMMA plate and PMMA cylinder [27]. The cylinder has the shape of a tube with a diameter of 1 m. The case study calculation assumes that the patient is located at a distance of 350 cm to the radiation source. The scatter is positioned at an source–surface distance (SSD) of 300 cm. Fig. 4a shows the geometrical boundary conditions of the case study calculation.

The effective material thickness of the scatter was calculated in dependence of the considered location of exposition. As an area of exposition, a horizontal expansion of 80 cm was assumed. It was assumed that the distance be-

tween the outsides of the right and left arms is about 80 cm. Furthermore, for both geometries of scatter, a PMMA thickness of 1 cm was determined. As expected, the results of the case study calculation (see Fig. 4b) show for the cylindrical scatter that from the irradiation center to the outside, the effective scatter thickness increases. At 30 cm off-axis, the effective scatter thickness increases by 25% and at 40 cm by 68%. In contrast, the effective scatter thickness of the PMMA plate changes by a maximum of 0.7%. This means that for the use of a cylindrical scatter, it needs to be considered that at peripheral areas of the patient, a further reduced energy and thus a reduced penetration depth occurs. The body flanks of the patient will be irradiated by therapy beam at tangential line caused by the body geometry. Thereby, the effective penetration depth is reduced enormously. The use of a cylindrical scatter will reduce the therapy beam at peripheral body areas yet further. From this point of view, the use of a planar scatter seems advantageous.

Relative depth dose distribution

The determination of the depth dose distribution was carried out in the PMMA-plate phantom. The point of measurement in PMMA z_{PMMA} was corrected under consideration of the electron density relation to get the equivalent depth of water z_W:

$$z_w = 1.16 \cdot z_{PMMA} \tag{3}$$

First of all, it was shown that a comparison measurement with a PMMA-plate phantom results in the same values as the measurements with a water phantom. Measurements took place under standard conditions (electron energy: 6 MeV, field size: 20 cm × 20 cm, SSD = 100 cm) and their results are shown in Fig. 5a. It arises that the percentage depth dose (PDD) measurements in PMMA and in water show an exact match. Occurring deviations are limited to the first half of the dose buildup region and range by 2% at maximum. Thus, the differences are estimated to be negligibly small.

To generate a PDD curve at designated treatment conditions, the PMMA phantom was placed in the patient's position. The point of measurement is located 15 cm behind a 1-cm thick PMMA plate. Also, the other parameters of the beam correlate with the real treatment situation (HDRE: 6 MeV, field size: 40 cm × 40 cm, SSD = 350 cm). While working with the HDRE mode, an open field without any conventional electron applicator collimation is used. Showing the impact of the larger SSD of 350 cm as well as effects of the 1-cm thick PMMA plate, measurements with and without a PMMA plate were performed at an SSD of 100 cm additionally to the measurements in the treatment situation (see Fig. 5b). The chief cause of the
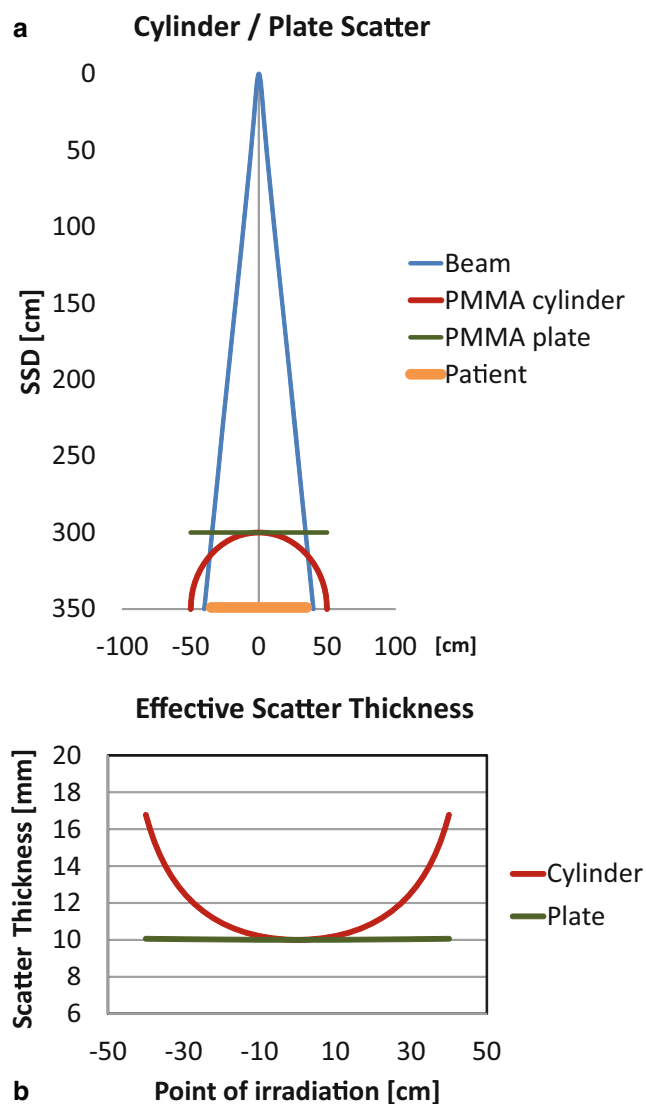
Fig. 4 Investigation of scatter. **a** Model for estimation of effective scatter thickness. **b** Effective scatter thickness depending on localization of exposition
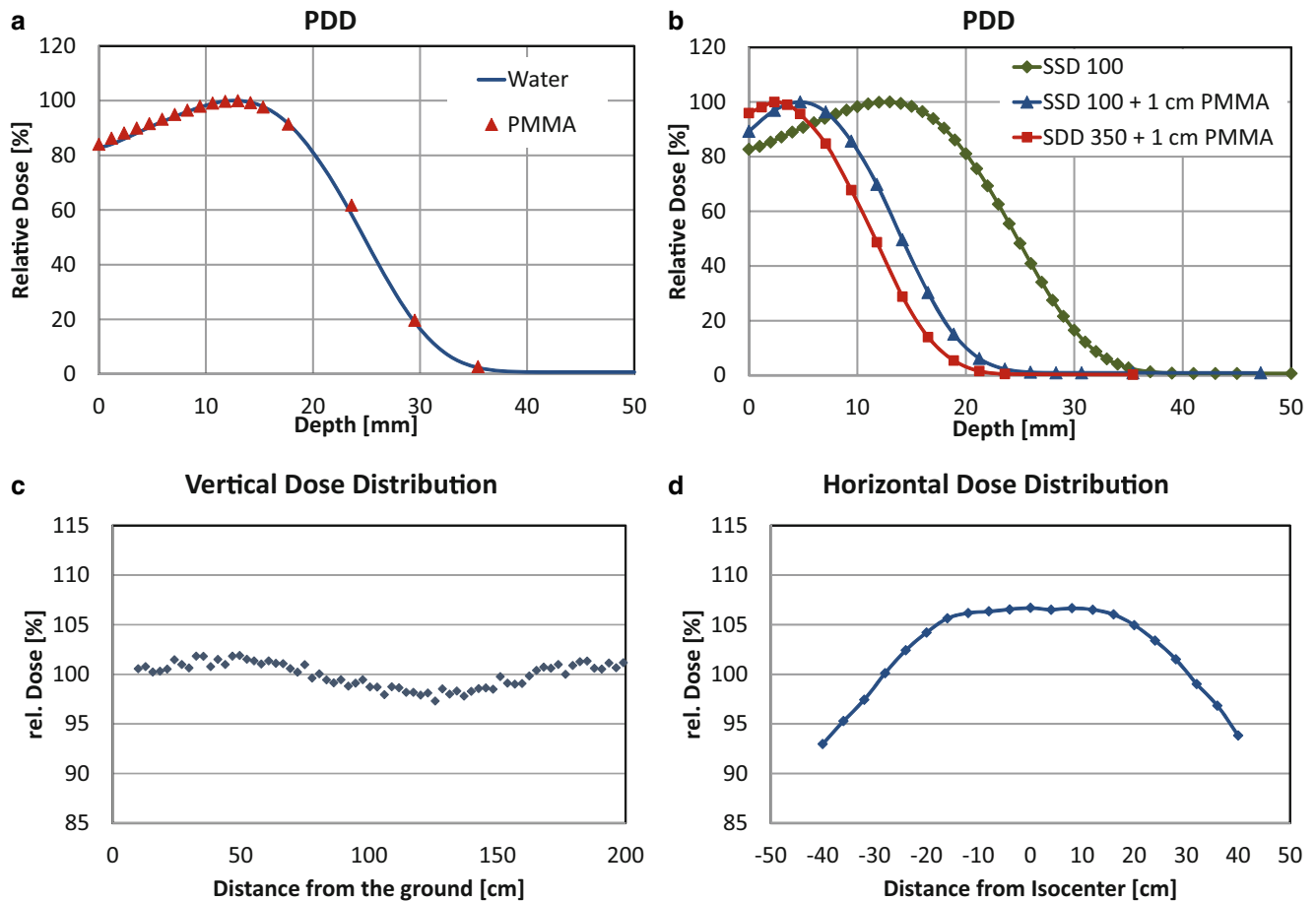
Fig. 5 Dose distribution. **a** Comparison of PDD distributions measured in water and in PMMA. **b** PDD distributions in treatment conditions in comparison with deviating conditions. **c** Vertical dose distribution. **d** Horizontal dose distribution

decrease of electron energy is implementation of the 1-cm thick PMMA plate, which serves as a scatter. A smaller part of this decrease is caused by the larger distance to the radiation source with a 350-cm SSD.

The outcomes of the PDD distribution corresponding to the treatment situation (SSD = 350 cm + 1 cm PMMA) are the following parameters, which are essential for the treatment:

- the therapeutic depth (80% of the prescription dose) amounts to R80 = 8 mm,
- the contamination of photons falls to below 1%,
- the depth at 50% of the maximum dose is R50 = 12 mm,
- the practical range is R_p = 18 mm,
- a mean electron energy of E = 3.2 MeV can be calculated using Eq. 4 [9].

$$E = 0.656 + 2.059 \cdot R50 + 0.022 \cdot R50^2 \, (MeV) \qquad (4)$$

The energy-dependent correction factor for absolute dosimetry k_E [3] rises consequently from 0.923 for 6 MeV to 0.951 for 3.2 MeV. This needs to be considered for determination of absolute dosimetry. The therapeutic depth

(80% of the prescription dose) could be reduced from 2 cm at an electron energy of 6 MeV to 0.8 cm. The PDD distribution also shows that placing a 3-cm thick PMMA plate as dose shielding additional to the 1-cm scatter results to an enormous dose reduction, to almost 0% remaining dose.

Vertical dose distribution

Ahead of the patient treatment, numerous studies were conducted with the aim of reaching a homogeneous dose distribution at a duration which is kept as short as possible. Therefore, the gantry angles of the arc field and both static fields as well as the monitor units were varied until an optimum solution was found. Roos chamber measurements were carried out, but these only give spot information about the whole vertical dose distribution. The potential irradiation area covers a good 2-m distance in the vertical direction. In order to achieve a sufficient resolution of dose distribution for vertical and horizontal dose profiles, measurements were carried out with radiochromic films. Fig. 5c shows the results of the vertical dose distribution, which corresponds to the vertical profile of the patient. The films

show that a homogeneous dose was achieved through optimization of the treatment fields. The dose varies by only ±2% over the whole vertical area.

Horizontal dose distribution

The horizontal dose profiles were measured at four different heights. Starting at the ground, the measurement heights were 20 cm, 70 cm, 120 cm (isocentre), and 170 cm. The measured dose profiles were almost congruent at all measurement heights. The horizontal dose profile is presented in Fig. 5d. It was measured for a potential therapeutic field size of 80 cm. The dose varies by about ±8% in this area. For a field size of 60 cm, the width of variation reduces to ±5%. Through experimental research with special PMMA scatters which were attached directly to the electron applicator, a homogeneous horizontal dose distribution could be achieved. These scatters were produced out of 2-mm thick PMMA plates of different sizes. The maximum material thickness was 10 mm. The application of such an additional scatter would cause an effect on the electron energy and thus it results to a location-dependent therapeutically depth. For this reason, the PMMA application was not used as additional scatter.

Absolute dose and film dosimetry

Initially, reference measurements with the water phantom were performed to prove the impact of the PMMA phantom on the measured absolute dose. The measurements at the water phantom took place under standard conditions according to DIN [3]. The depth of measurement for the PMMA phantom was corrected corresponding to the PMMA electron density (Eq. 3). The factor for dose correction was determined as 0.95. It is necessary to apply this additional correction factor because for phantom measurements, the energy-dependent correction factor k_E (see DIN [3]) is not taken into account.

Results of in situ dosimetry

Irradiation of the patient takes place with an orientation of the patient to the gantry of 0°, 120°, and 240° on day 1 and 60°, 180°, and 300° on day 2. The purpose of this approach is to preferably irradiate all parts of the body frontally as well as laterally by the therapy beam. Whereas the tangentially reached areas of skin are exposed by each of the neighboring beams, the dose to the skin parts which are towards the beam source are largely only reached by one beam. The in situ measurements confirm this view. Fig. 6a reveals that the skin doses depending on the respective position to the beam source vary by a factor of up to 2.
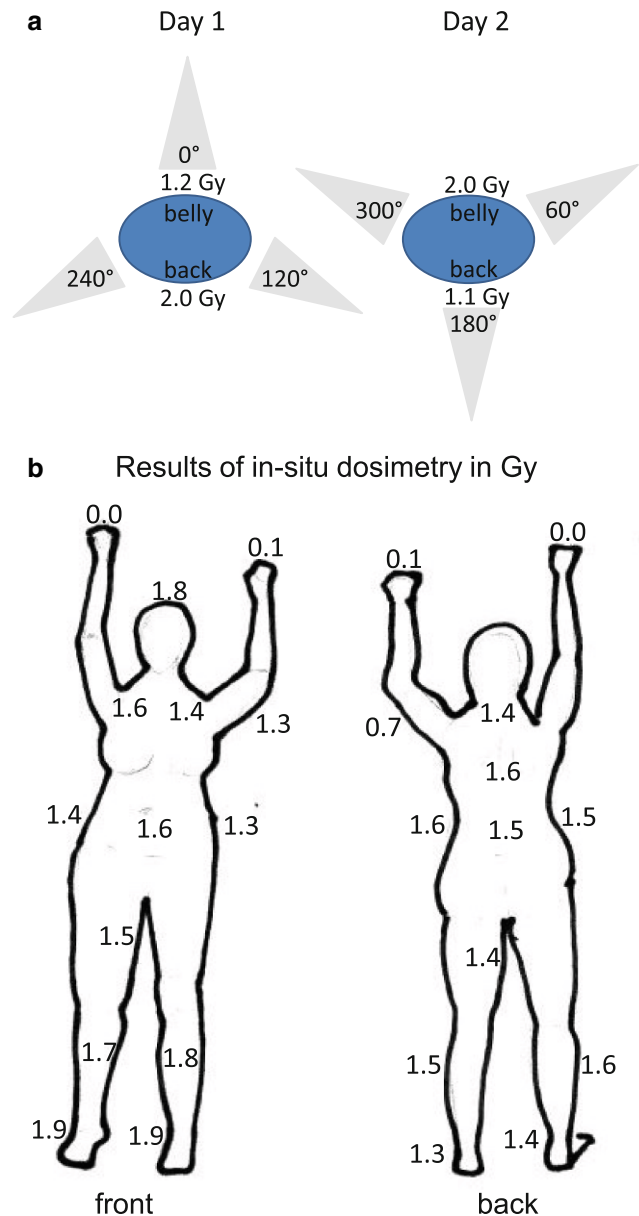
Fig. 6 In situ dosimetry. **a** Results measured by in situ dosimetry for irradiation setup including treatment angles on different days. **b** Results of in situ dosimetry for specific spots

Due to the daily change of patient position with respect to the irradiation source, a relatively homogeneous mean dose distribution can be achieved.

At 8 days of treatment, in total, 69 in situ measurements of the skin dose were accomplished exemplarily. Dose values of each spot of exposition were averaged over the measurement days and thus comply with the mean dose of the respective skin parts. The results of the in situ measurements are shown in Fig. 6b. The highest doses are measured at the instep of the foot. This is in line with expectations, as independent of the respective patient orientation, the instep

is exposed by several beams at each fraction. The fractional dose was chosen not to exceed the maximum dose of 2.0 Gy. In order to maintain this boundary with certainty, the dose of the instep was measured at all measurement days. The areas of the shoulder also receive dose fractions of at least two beams, but they are exposed more tangentially than frontally. With 1.4 and 1.6 Gy, the mean doses of the shoulder areas are lower than the mean dose of the instep of the foot at 1.9 Gy. The lowest doses are determined at the inner side of the upper arm with 0.7 Gy, which correlates with dose measurements in the literature [6].

The remaining measurements reveal that mean doses to the torso as well as to the extremities, with values between 1.3 and 1.8 Gy, are relatively homogeneous.

Discussion

Techniques for TSEBT which are applied today show similarities in many ways. Differences exist in irradiation time and in the homogeneity of dose profiles. Both probably don't have an influence on the therapy.

Perhaps a substantial difference results from using different scatters, which are used for homogeneous dose distributions. In the literature, various shapes of scatter are presented in relation to TSEBT. These can, in principle, be distinguished by scatters with constant material thickness [17] and scatters with different material thicknesses [8]. Furthermore, in some radiation centers, scatters are installed next to the radiation source and others prefer a scatter position next to the patient.

The investigations have shown that for determination of dose as well as for determination of penetration depth, a relatively high measurement effort is necessary. Particularly with the application of scatters, it needs to take the changes in energy of the electron beam both for determination of skin dose and estimation of the penetration depth into account. The use of a scatters with different material thicknesses increases the measurement uncertainty for determination of the actually achieved skin dose.

Conclusion

Total skin irradiation with electrons in a sweeping-beam technique is a safe and reproducible technique, with a homogeneous vertical and horizontal dose distribution. These findings were verified both in vitro and in vivo measurements on phantoms and patients. In addition, the patients benefit from a very short treatment time.

References

1. Asbell SO, Siu J, Lightfoot DA, Brady LW (1980) Individualized eye shields for use in electron beam therapy as well as low-energy photon irradiation. Int J Radiat Oncol Biol Phys 6(4):519–521

2. Bin Xu L (2009) Commissioning of a GafChromic EBT film dosimetry protocol at ionizing radiation standards group of National Research Council

3. DIN 6800-2. Dosismessverfahren nach der Sondenmethode für Photonen- und Elektronenstrahlung – Teil 2: Dosimetrie hochenergetischer Photonen- und Elektronenstrahlung mit Ionisationskammern. 2020;

4. Earley L, Moeller J, O'Rear J, Leavitt DD (1995) A method for total skin electron treatment for infants. Med Dosim 20(4):243–248

5. Elsayad K, Kroeger K, Greve B et al (2020) Low-dose total skin electron beam therapy: Quality of life improvement and clinical impact of maintenance and adjuvant treatment in patients with mycosis fungoides or Sezary syndrome. Strahlenther Onkol 196(1):77–84

6. Elsayad K, Moustakis C, Simonsen M, Bäcker D, Haverkamp U, Eich HT (2018) In-vivo dosimetric analysis in total skin electron beam therapy. Phys Imaging Radiat Oncol 6:61–65 (www.sciencedirect.com/science/article/pii/S2405631617300829)

7. Elsayad K, Stadler R, Steinbrink K, Eich HT (2020) Combined total skin radiotherapy and immune checkpoint inhibitors: a promising potential treatment for mycosis fungoides and Sezary syndrome. Dtsch Dermatol Ges 18(3):193–197

8. Evans MDC, Hudon C, Podgorsak EB, Freeman CR (2014) Institutional experience with a rotational total skin electron irradiation (RTSEI) technique—A three decade review (1981–2012). Rep Pract Oncol Radiother 19(2):120–134

9. Gerbi BJ, Antolak JA, Deibel FC et al (2009) Recommendations for clinical electron beam dosimetry: supplement to the recommendations of Task Group 25. Med Phys 36(7):3239–3279

10. Hensley FW, Major G, Edel C, Hauswald H, Bischof M (2014) Technical and dosimetric aspects of the total skin electron beam technique implemented at Heidelberg University Hospital. Rep Pract Oncol Radiother 19(2):135–143

11. Jones GW, Kacinski BM, Wilson LD et al (2002) Total skin electron radiation in the management of mycosis fungoides: Consensus of the European Organization for Research and Treatment of Cancer (EORTC) Cutaneous Lymphoma Project Group. J Am Acad Dermatol 47(3):364–370

12. Kalef-Ezra J, Karava K (2008) Radiochromic film dosimetry: reflection vs transmission scanning. Med Phys 35(6 Part 1):2308–2311

13. Karzmack CJ, Anderson J, Fessenden P et al (1987) AAPM report No. 23, total skin electron therapy: technique and dosimetry, vol 30. Rep Gr

14. Koylu M, Kamer S, Anacak Y, Yalman D (2020) Development of an intensity modulated total skin electron irradiation technique. Int J Radiat Oncol. https://doi.org/10.1016/j.ijrobp.2020.07.742

15. Krieger H (2001) Strahlenphysik, Dosimetrie und Strahlenschutz, 3rd edn. Teubner, Stuttgart

16. Kroeger K, Elsayad K, Moustakis C, Haverkamp U, Eich HT (2017) Niedrigdosis-Ganzhautelektronenbestrahlung bei Patienten mit kutanen Lymphomen: Minimales Risiko für akute Toxizitäten. Strahlenther Onkol 193(12):1024–1030

17. Licona I, Figueroa-Medina E, Gamboa-deBuen I (2017) Dose distributions and percentage depth dose measurements for a total skin electron therapy. Radiat Meas 106:365–372

18. Mazzeo E, Rubino L, Buglione M et al (2014) The current management of mycosis fungoides and Sezary syndrome and the role of radiotherapy: principles and indications. Rep Pract Oncol Radiother 19(2):77–91

19. Müller-Sievers K, Ertan E, Kober B (2001) Dosimetry of rotational partial-skin electron irradiation. Radiother Oncol 58(2):187–192

20. Park S-Y, Ahn BS, Park JM, Ye S-J, han Kim I, Kim J (2014) Dosimetric comparison of 4 MeV and 6 MeV electron beams for total skin irradiation. Radiat Oncol 9(1):1–6

21. Piotrowski T, Milecki P, Skórska M, Fundowicz D (2013) Total skin electron irradiation techniques: a review. Adv Dermatol Allergol 30(1):50

22. Poli MER, Todo AS, Campos LL et al (2010) Dose measurements in the treatment of mycosis fungoides with total skin irradiation using a 4 meV electron beam. Instituto de Pesquisas Energéticas e Nucleares: P-7-68

23. Reinhardt S, Hillbrand M, Wilkens JJ, Assmann W (2012) Comparison of Gafchromic EBT2 and EBT3 films for clinical photon and proton beams. Med Phys 39(8):5257–5262

24. Reynard EP, Evans MDC, Devic S et al (2008) Rotational total skin electron irradiation with a linear accelerator. J Appl Clin Med Phys 9(4):123–134

25. Rolf D, Elsayad K, Eich HT (2020) Ultra-hypofractionated low-dose total skin electron beam followed by maintenance therapy: preliminary findings from a prospective open-label study. J Am Acad Dermatol. https://doi.org/10.1016/j.jaad.2020.11.058

26. Rudat V, Nour A, Alaradi AA, Mohamed A, Altuwaijri S (2014) In vivo surface dose measurement using GafChromic film dosimetry in breast cancer radiotherapy: comparison of 7-field IMRT, tangential IMRT and tangential 3D-CRT. Radiat Oncol 9(1):1–9

27. Schüttrumpf L, Neumaier K, Maihoefer C et al (2018) Dose optimization of total or partial skin electron irradiation by thermoluminescent dosimetry. Strahlenther Onkol 194(5):444–453

28. Trautinger F, Knobler R, Willemze R et al (2006) EORTC consensus recommendations for the treatment of mycosis fungoides/Sézary syndrome. Eur J Cancer 42(8):1014–1030

29. Wu J-M, Leung SW, Wang C-J, Chui C-S (1997) Lying-on position of total skin electron therapy. Int J Radiat Oncol Biol Phys 39(2):521–528

30. Yousif YAAM (2007) Commissioning and optimization of a total skin electron therapy technique using a high rate electron facility. PhdThesis, University of the Free State